

Hard sphere-like dynamics in a non hard sphere liquid

T. Scopigno^{1,2}, R. Di Leonardo^{1,2}, L. Comez^{1,3}, A.Q.R. Baron⁴, D. Fioretto^{1,5}, G. Ruocco^{1,6}

¹*INFN CRS-SOFT, c/o Università di Roma "La Sapienza", I-00185, Roma, Italy*

²*INFN UdR-RS, c/o Dipartimento di Fisica, Università di Roma "La Sapienza", I-00185, Roma, Italy*

³*INFN UdR-PG, c/o Dipartimento di Fisica, Università di Perugia, via Pascoli, I-06123 Perugia, Italy*

⁴*SPRING-8/JASRI, 1-1-1 Kouto, Mikazuki-cho, Sayo-gun, Hyogo-ken 679-5198 Japan.*

⁵*Dipartimento di Fisica, Università di Perugia, via Pascoli, I-06123 Perugia, Italy*

⁶*Dipartimento di Fisica, Università di Roma "La Sapienza", I-00185, Roma, Italy.*

(Dated: August 15, 2018)

The collective dynamics of liquid Gallium close to the melting point has been studied using Inelastic X-ray Scattering to probe lengthscales smaller than the size of the first coordination shell. Although the structural properties of this partially covalent liquid strongly deviate from a simple hard-sphere model, the dynamics, as reflected in the quasi-elastic scattering, are beautifully described within the framework of the extended heat mode approximation of Enskog's kinetic theory, analytically derived for a hard spheres system. The present work demonstrates the applicability of Enskog's theory to non hard- sphere and non simple liquids.

PACS numbers: 67.40.Fd, 05.20.Dd, 67.55.Jd, 61.10.Eq

Since the first appearance of Enskog's theory [1], special attention has been devoted to the theoretical and numerical study of the dynamics of hard spheres fluid as a useful tool to mimic the behavior of simple liquids [2, 3]. During the seventies, the development of neutron scattering (INS) facilities provided a database of dynamical properties of simple liquids, while the enormous advances of computational capabilities allowed recourse to the hard sphere model to evaluate transport coefficients [4] and neutron scattering response [5]. At the same time, on the theoretical side, the dynamical properties of an ensemble of hard spheres have been investigated by revisiting Enskog's original kinetic theory. One of the most significant outcomes of these efforts is the so called extended hydrodynamic theory [6, 7, 8, 9], which has been particularly successful in describing INS data [10]. While Enskog's kinetic theory, strictly speaking, applies to hard spheres fluids only, it has the advantage of readily predicting the Q -dependence of some transport coefficients, as opposed to more rigorous and involved theories using memory functions or generalized hydrodynamics. Thus this theory remains a very useful tool.

The extent of validity of Enskog's kinetic approach has been satisfactorily tested against inelastic neutron scattering data collected in very simple liquids including Kr, Ar, Ne, Rb [10]. These are all similar in that their structure is well described by a hard sphere model, with an effective density and radius which can be determined by matching the first peak of the static structure factor. However, no attempt has been made, to our knowledge, to verify the applicability of the theory to liquids markedly deviating from hard-sphere like structures, probably because very few accurate, constant Q , experimental determination of coherent spectra exist in these systems [11].

In this letter, we present a study of the collective dynamic structure factor ($S(Q, \omega)$) at wavevectors beyond

the first maximum of the static structure factor ($S(Q)$), using inelastic x-ray scattering. The system we address is liquid gallium, as the purpose of this work is to ascertain validity of the connection between structural and dynamical properties as predicted by Enskog's hard sphere theory for a liquid with strong non-hard- sphere structural properties. Among simpler liquids, Ga has peculiar structural and electronic properties. In addition to the low melting temperature ($T_m = 303$ K), it shows an extended polymorphism in the solid phase with complex crystal structures characterized by the competition between metallic and covalent bindings. Despite the nearly free electron electronic DOS, anomalies associated with some covalency residue have been reported [12]. Among them, the most important for the present purpose is that the first peak of the $S(Q)$ presents a hump characteristic of non close-packed liquid structures [13, 14], which marks a significant departure from the smoother behavior of the hard sphere structure factor. Although the dynamics of liquid Gallium has been previously studied by INS [15, 16, 17] and IXS [18], the restricted available Q range in the first case, and the presence of incoherent scattering in the second case, prevented a study of the collective dynamics in a Q region beyond the main peak of the structure factor like the present one.

We demonstrate that the collective dynamics of molten gallium is well described by Enskog theory up to wavevectors as large as three times that of the first maximum of the static structure factor. While the reduced density and mean free path of liquid Gallium at melting point fall into the region of applicability of Enskog's theory, the structural peculiarities of this system would discourage any recourse to predictions stemming from a hard sphere paradigm. However, the hard-sphere model turns out to describe the dynamics even in the region where the structure factor is notably different than a hard-sphere model.

The experiment was performed at the high resolution inelastic scattering beam-line (BL35XU) [19] of SPring-8 in Hyogo prefecture, Japan. High resolution was obtained using the (9 9 9) reflection of perfect silicon crystals while a backscattering geometry ($\frac{\pi}{2} - \theta_B \approx 0.3$ mrad) was used (for both monochromator and analyzers) in order to obtain large angular acceptance. The flux onto the sample was $\approx 10^{10}$ photons/sec (100 mA electron beam current) in a 1.8 meV bandwidth at 17.793 keV. The use of 4 analyzer crystals, placed with 0.70 degree spacing on the 10 m two-theta arm (horizontal scattering plane), and 4 independent detectors, allowed collection of 4 momentum transfers simultaneously. Slits in front of the analyzer crystals limited their acceptance to 0.24 nm^{-1} in the scattering plane. The over-all resolution of the spectrometer was about 2.8 meV, depending on the analyzer crystal. Typical data collection times were 200 s/bin, where the bin size was fixed at 0.25 meV.

The Ga sample, about 80 microns in thickness, was placed in sample cell with thin (2×250 micron) single crystal sapphire windows. This was held, in vacuum, at a constant temperature of 315 K.

Measured IXS spectra are reported in Fig. 1 for selected constant values of momentum transfer Q . The strong central peak is readily visible along with some background due to phonons in the sapphire windows. Solid lines in the figure are best-fits with two components: *i*) a single Lorentzian line, modified in the usual way to account for detailed balance [20], and convolved with the instrumental resolution and *ii*) the empty cell background measured at each Q , normalized by the sample transmission. As it will be shown in the following, the Lorentzian spectrum is predicted by Enskog's kinetic theory, which also furnishes explicit expressions for the Q -dependence of the parameters describing its linewidth and amplitude (see, for instance, Eq. (5)).

The main idea behind Enskog's theory is to evaluate the correlation functions of the microscopic quantities, such as the density-density correlation function of interest here, replacing the Liouville operator and the set of relevant dynamical variables defined at the N -particle ensemble level, with the one particle Enskog operator L and appropriate single particle variables. Within this framework, the dynamic structure factor reads ([6, 7, 8, 9]):

$$\begin{aligned} S(Q, \omega) &= S(Q) \frac{1}{\pi} \text{Re} \left\{ \left\langle \frac{1}{i\omega - L(\mathbf{Q}, \mathbf{v}_1)} \right\rangle_1 \right\} \\ &= S(Q) \frac{1}{\pi} \text{Re} \left\{ \sum_j \frac{B_j(Q)}{i\omega + z_j(Q)} \right\} \end{aligned} \quad (1)$$

with

$$B_j(Q) = \langle \Psi_j^{(L)}(\mathbf{Q}, \mathbf{v}_1) \rangle_1 \langle \Psi_j^{(R)*}(\mathbf{Q}, \mathbf{v}_1) \rangle_1 \quad (2)$$

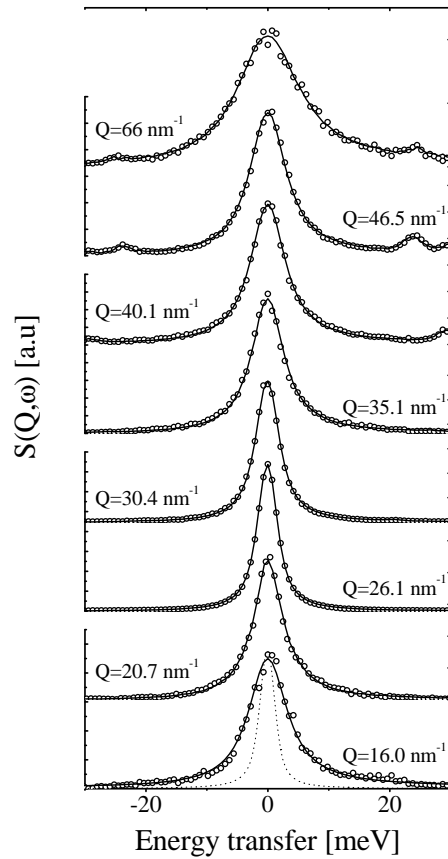


FIG. 1: IXS spectra of liquid Ga ($T = 315$ K) at the indicated fixed Q values (open dots). Also reported is the instrumental resolution (which is the same -dotted line- for all the reported spectra) and the best-fit lineshapes (continuous line, see text). The structures at larger energy transfers are phonons from the sapphire windows of the sample container.

The subscript $\langle \dots \rangle_1$ indicates a single particle averages over the Maxwell Boltzmann velocity distribution function, while $z_j(Q)$, $\Psi_j^{(L)}(\mathbf{Q}, \mathbf{v}_1)$ and $\Psi_j^{(R)}(\mathbf{Q}, \mathbf{v}_1)$ are the eigenvalues and the left and right eigenvectors of L , respectively.

There are several approaches to determine the spectrum of L , and different approximations can be applied depending on the density and kinematic regions of interest. Following Ref. [9], these regions are identified by the values of the reduced density

$$V_0/V = \rho\sigma^3/\sqrt{2} \quad (3)$$

in which V_0 is the closest packing volume for spheres of radius σ and number density ρ , and by Enskog's mean free path $l_E = l_0/\chi$, with $l_0 = 1/\sqrt{2}\rho\pi\sigma^2$ the Boltzmann mean free path and $\chi = g(\sigma)$ the pair distribution function evaluated at the contact point between two spheres.

Taking, as usual, density, momentum and energy as relevant variables, the lower three eigenvalues of L always

go to zero with $Q \rightarrow 0$. By introducing Enskog's thermal diffusion coefficient D_E , the adiabatic sound velocity c_o and the sound damping coefficient Γ_E , it can be shown that these low lying eigenvalues are [7, 8]:

$$\begin{aligned} z_1(Q) &= z_h(Q) = D_E Q^2 \\ z_{2,3}(Q) &= z_{\pm}(Q) = \pm i c_o Q + \Gamma_E Q^2 \end{aligned} \quad (4)$$

This limit is practically attained at low densities ($V_0/V < 0.1$ and therefore $l_E \approx l_0$) and sufficiently small Q 's ($Q\sigma \ll 1$). This condition normally occurs in the case of light scattering experiments from dilute gases ($Ql_0 \approx 1$), and one speaks in terms of three extended hydrodynamic modes.

In dense fluids (V_0/V approximately larger than 0.35), Kamgar-Parsi et al. have shown that a description in terms of three *effective* hydrodynamic modes still applies [9], and the low Q limit of these modes is again coincident with the hydrodynamic result. At variance with the previous case, however, the hydrodynamic scheme breaks down as soon as $Ql_E \approx 0.05$. Above this value, Enskog's operator is dominated by binary collisions and only the extended heat mode is well separated by all the other modes [9]. The following approximate expression for the extended heat mode can be given:

$$z_h(Q) = \frac{D_E Q^2}{S(Q)} d(Q) \quad (5)$$

in which D_E is Enskog diffusion coefficient and

$$d(Q) \approx \frac{1}{1 - j_0(Q\sigma) + 2j_2(Q\sigma)} \quad (6)$$

can be expressed in terms of the first two even order Bessel spherical functions. Enskog's diffusion coefficient is related to the Boltzmann diffusion coefficient

$$D_0 = \frac{3}{8\rho\sigma^2} \sqrt{\frac{k_B T}{\pi m}} \approx \frac{0.216}{\rho\sigma^2} \sqrt{\frac{k_B T}{m}}$$

by the collision enhancing term $g(\sigma)$ as $D_E = D_0/g(\sigma)$. Plugging the well known analytic expression of $g(\sigma)$ for hard spheres [21] in the previous equation, one easily gets a final expression for D_E in terms of the packing fraction $\varphi = \pi\rho\sigma^3/6$:

$$D_E = \frac{1}{16} \sqrt{\frac{\pi k_B T}{m}} \sqrt[3]{\frac{6}{\pi\rho\varphi^2} \frac{(1-\varphi)^3}{(1-\varphi/2)}} \quad (7)$$

Summing up, by virtue of the results recalled sofar, the $S(Q, \omega)$ in dense fluids, such as in the present case of a monoatomic liquid close to the melting point, can be described to a sufficient extent of accuracy in terms

of three Lorentzian lines (effective hydrodynamic modes) up to relatively large wavevectors ($Q \approx 20 \text{ nm}^{-1}$), while above this value the acoustic mode is overdamped and the quasi-elastic extended heat mode should dominate ($Ql_E \gg 0.05$). The full width at half maximum (FWHM) of the quasi-elastic mode is quantitatively predicted by Eq.s (5), (6) and (7).

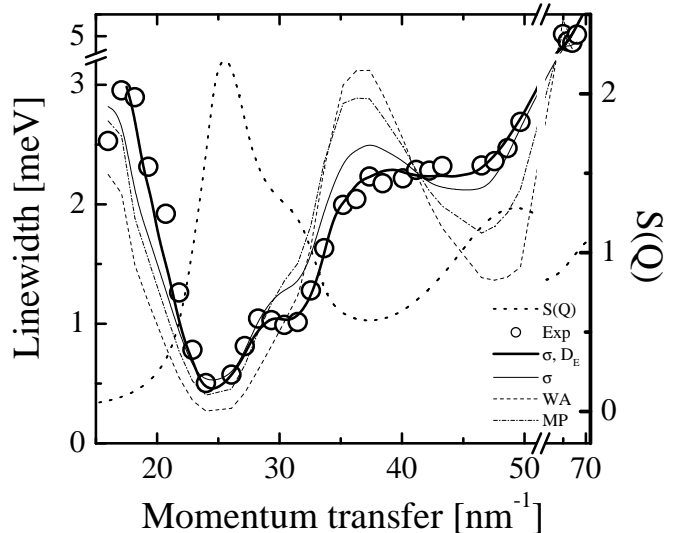


FIG. 2: FWHM of the dynamic structure factor (left axis): experimental determination (open circles, error bars smaller than the symbol size) and different predictions according to the revised Enskog's theory (Eq.(5)). Thin continuous line: σ is the only fitting parameter (D_E is determined exploiting Eq.(7)). Thick continuous line: both σ and D_E are fitting parameters. Thin dashed line (WA): σ is determined as the value corresponding to the hard sphere structure factor which better describes the measured $S(Q)$ (D_E is the only fitting parameter). Thin dot-dashed line (MP): σ is determined from the main peak of the structure factor, through Eq.(8) (D_E is the only fitting parameter). Also reported is the static structure factor (dotted line, right axis), which drives the oscillations in the FWHM.

The half width at half maximum of the quasi-elastic line (heat mode) are reported in Fig. 2 as a function of the Q values, together with the $S(Q)$ [14]. Here, one can clearly observe oscillations in the line-width driven by the $S(Q)$. The second minimum at $Q \approx 30 \text{ nm}^{-1}$, in particular, is clearly related to the shoulder of the $S(Q)$ observed the same Q position. The line-width predicted by Eq.(5) is also reported, with different choices of the two parameters σ and D_E (see table I). By leaving both parameters free one gets a best fit value of $\sigma = 0.279 \text{ nm}$, corresponding to a packing fraction of $\varphi = 0.601$ (and a reduced density $V_0/V = 0.811$) which is just beyond the maximum theoretical value for hard spheres ($\varphi = 0.545$). This seems to be a reasonable result for a dense liquid, like the one under investigation here, recalling that σ has to be regarded to as an effective parameter, thus not necessarily *strictly* related to the density through Eq. (3).

Using only σ as free parameter (i.e. exploiting Eq.(7)) one still gets reasonable agreement (thin continuous line in Fig.2), even in the region of the secondary shoulder.

Aiming at a description of microscopic properties of a simple fluid within the hard sphere paradigm, alternative choices of the effective particle diameter can be considered. One can, indeed, choose σ from the position of the first peak Q_M of the structure factor [10] (MP):

$$\sigma = \frac{2\pi}{Q_M} \quad (8)$$

or, through Eq.(3), by adjusting the value of the reduced density to maximize the whole $S(Q)$ agreement [22] (WA). We tried both, either using Eq.(7) or not, and the agreement with the experimental line-width is poor. The results are quantitatively summarized in table I: by fixing the hard- sphere diameter with one of the two mentioned criteria the χ^2 is definitely worse. Moreover, looking at Fig.(2), one clearly observes that with this choices the secondary minimum observed in the FWHM at $Q \approx 30 \text{ nm}^{-1}$ is smeared out. This feature, therefore, is not the mere consequence of the oscillations in $S(Q)$ (De Gennes narrowing). It testifies to the presence of hard sphere dynamics and allows the sharp determination of an effective hard sphere diameter via the Bessel terms of Eq.(5).

But what is the physical meaning of such "dynamical" effective diameter, and why it is larger than those obtained from the static structure factor? As we already mentioned, a description in terms of a uniform distribution of hard spheres does not apply to liquid gallium, as well as to several other liquid metals (Zn, Cd, Bi, Si). The covalency residue of Ga, in particular, has been rationalized in terms of dimer-like structures [12], and clustering effects have been hypotized aiming to reproduce the $S(Q)$ [22]. The effective diameter that we find, therefore, could be an indication of the supra-atomic nature of the "effective particles". Consistently, plugging our effective $\sigma = 0.279 \text{ nm}$ in Eq. (7), and solving it for a correspondent effective mass, we get $m_{eff} = 83 \text{ a.m.u.}$, which is larger than the atomic mass of gallium $m = 69.7 \text{ a.m.u.}$ The effective mass and diameter, therefore, could be regarded as the mean sizes of the "clusters" undergoing collective dynamics. This hypothesis, however, needs to be tested extending the present study to other systems and at different temperature, as the structural anomalies are known to be strongly temperature dependent.

In summary, we have shown how the microscopic dynamics of a well known non hard-sphere liquid, namely liquid Gallium at the melting point, is surprisingly well described by Enskog's theory, analytically derived for a hard-sphere fluid. More specifically, the connection between structure and dynamics, which is the main outcome of this theory, is robust enough to persist even in a wavelength region where anomalies typical of non simple

liquids develop. From the experimental data, therefore, an *effective* hard-sphere diameter can be obtained, which turns out to be larger than the one related to structural properties according to well established methods. This result suggests, therefore, an extended validity of the revised Enskog's theory beyond the class of systems (hard spheres) for which it was derived, and provides an experimental route to the determination of an *effective dynamical* diameter.

The authors are grateful to P. Ascarelli, E. G. D. Cohen, F. Sciortino and J.-B. Suck for fruitful discussions. The synchrotron radiation experiment was performed at the SPring-8 with the approval of the Japan Synchrotron Radiation Research Institute (JASRI) (Proposal No. 2004A0634-ND3d-np).

-
- [1] S. Chapman and T. Cowling, *The mathematical theory of non uniform gases* (1952).
 - [2] J. L. Lebowitz, J. K. Percus, and J. Sykes, Phys. Rev. **188**, 487 (1969).
 - [3] P. M. Furtado, G. F. Mazenko, and S. Yip, Phys. Rev. A **12**, 1653 (1975).
 - [4] W. E. Alley, B. J. Alder, and S. Yip, Phys. Rev. A **27**, 3174 (1983).
 - [5] W. E. Alley and B. J. Alder, Phys. Rev. A **27**, 3158 (1983).
 - [6] I. M. de Schepper and E. G. D. Cohen, Phys. Rev. A **22**, 287 (1980).
 - [7] I. M. de Schepper, E. G. D. Cohen, and M. J. Zuilhof, Phys. Lett. **101A**, 399 (1984).
 - [8] E. G. D. Cohen, I. M. de Schepper, and M. J. Zuilhof, Physica **127B**, 282 (1984).
 - [9] B. Kamgar-Parsi, E. G. D. Cohen, and I. M. de Schepper, Phys. Rev. A **35**, 4781 (1987).
 - [10] E. G. D. Cohen, P. Westerhuijs, and I. M. de Schepper, Phys. Rev. Lett. **59**, 2872 (1987).
 - [11] U. Dahlborg and L. G. Olsson, Phys. Rev. A **25**, 2712 (1982).
 - [12] X. G. Gong, G. L. Chiarotti, M. Parrinello, and E. Tosatti, Phys. Rev. B **43**, R14277 (1991).
 - [13] P. Ascarelli, Phys. Rev. B **143**, 36 (1966).
 - [14] M. C. Bellissent-Funel, P. Chieux, D. Levesque, and J. J. Weis, Phys. Rev. A **39**, 6310 (1989).
 - [15] F. J. Bermejo, M. Garcia-Hernandez, J. L. Martinez, and B. Hennion, Phys. Rev. E **49**, 3133 (1994).
 - [16] F. J. Bermejo, R. Fernandez-Perea, M. Alvarez, B. Roessli, H. E. Fischer, and J. Bossy, Phys. Rev. E **56**, 3358 (1997).
 - [17] L. E. Bove, F. Formisano, F. Sacchetti, C. Petrillo, A. Ivanov, B. Dorner, and F. Barocchi, Phys. Rev. B **71**, 014207 (2005).
 - [18] T. Scopigno, A. Filipponi, M. Krisch, G. Monaco, G. Ruocco, and F. Sette, Phys. Rev. Lett. **89**, 255506 (2002).
 - [19] A. Q. R. Baron, Y. Tanaka, S. Goto, K. Takeshita, T. Matsushita, and T. Ishikawa, J. Phys. Chem. Solids **61**, 461 (2000).
 - [20] T. Scopigno, U. Balucani, G. Ruocco, and F. Sette, J.

- Phys. C **12**, 8009 (2000).
- [21] T. Faber, *Introduction to the Theory of Liquid Metals* (Cambridge University Press, Cambridge, 1972).
- [22] S. F. Tsay and S. Wang, Phys. Rev. B **50**, 108 (1994).

σ	D_E	χ^2	σ [nm ⁻¹]	$\hbar D_E$ [meV/nm ⁻²]	Packing fraction $\varphi = \frac{\pi}{6}\rho\sigma^3$	Reduced density $V_0/V = \rho\sigma^3/\sqrt{2}$	l_E [nm]
FREE	FREE	46	0.279	1.14×10^{-3}	0.601	0.811	9.32×10^{-3}
FREE	Eq.(7)	108	0.265	1.13×10^{-3}	0.513	0.693	9.24×10^{-3}
MP	FREE	353	0.246	1.09×10^{-3}	0.411	0.555	8.90×10^{-3}
MP	Eq.(7)	4988	0.246	2.18×10^{-3}	0.411	0.555	1.78×10^{-2}
WA	FREE	681	0.226	9.54×10^{-4}	0.318	0.430	7.78×10^{-3}
WA	Eq.(7)	38533	0.226	3.78×10^{-3}	0.318	0.430	3.08×10^{-2}

TABLE I: Structural and dynamical properties of liquid gallium at the melting point, as derived by the present experiment. Each row is relative to a different fitting strategy, since the effective hard sphere diameter has been determined: *i*) as an adjustable parameter, *ii*) by the position of the main peak of the structure factor (MP), *iii*) as the value corresponding to the hard sphere structure factor which better approximates the measured one (WA). Correspondingly, the Enskog's diffusion coefficient, D_E , can be obtained either as an additional adjustable parameters or fixed through Eq.(7). All the other quantities are derived by σ and D_E according to the definitions given in the text.